Journal of
Water & Climate Change

IWA PUBLISHING

Journal of Water and Climate Change Vol 14 No 12, 4860 doi: 10.2166/wcc.2023.556

The hidden consequences of sea level rise: assessing vulnerability of buried infrastructure to groundwater inundation in American Samoa

Christopher Shuler

University of Hawaii at Manoa Water Resources Research Center and Hawaii Sea Grant College Program, Honolulu, Hawaii, USA
E-mail: cshuler@hawaii.edu

CS, 0000-0001-5259-6684

ABSTRACT

To island nations, sea level rise (SLR) is an existential threat. An insidious and often hidden consequence of SLR is groundwater inundation (GWI), which reduces the unsaturated zone causing flooding, enhanced corrosion, and reduced service life of buried utilities. In the Pacific, SLR may reach 0.6–2.5 m by the end of century, and on Tutuila, American Samoa (AS), apparent SLR is five times the global average, making adaptation planning critically important. This study addresses the climate impact-knowledge-gap regarding AS's infrastructure by combining a numerical groundwater model with buried and surface utility data to map where adaptation efforts should be prioritized. Rigorous studies of GWI are few, and this study is the first to model this phenomenon in the South Pacific. The model estimates that 70 km or 45% of the buried water, electrical, and sewer lines will be inundated, and 28% of present-day roads, 13.6% of buildings, and 20% of water-booster stations will be permanently flooded under a 2.4-m SLR scenario with projected recharge in 2100. These effects are often overlooked by or unknown to policy and decision makers; therefore, building awareness of GWI will help managers in AS and in other island communities to prioritize holistic adaptation actions.

Key words: American Samoa, groundwater inundation, groundwater modeling, infrastructure, sea level rise, tropical island

HIGHLIGHTS

- Groundwater inundation (GWI), a lesser known consequence of sea level rise (SLR), threatens buried infrastructure in island nations.
- American Samoa faces significant inundation of buried (45%) and surface (28%) infrastructure at 2.4-m SLR.
- This study, the first of its kind in the South Pacific, helps prioritize areas most vulnerable to GWI and emphasizes the need for climate adaptation in island communities.

GRAPHICAL ABSTRACT

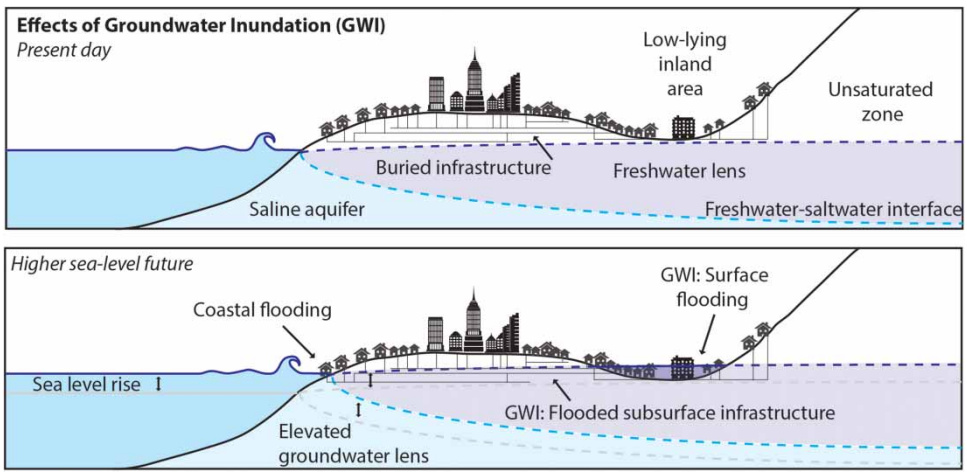

1. INTRODUCTION

Over 625 million island residents reside in low-elevation coastal zones across the globe. Future sea level and flood model projections suggest that within a decade, over 30% of these people will live within the 100-year flood plain (Neumann *et al.* 2015). Many of these vulnerable populations are served by an extensive network of surface-based and subsurface infrastructure, which is particularly at risk to impacts of sea level rise (SLR). In the Western Pacific Ocean, regional sea levels have been rising at a rate of 3.2 mm/year since the 1990s (Hamlington *et al.* 2014). Like many tropical islands across the globe, the U.S. Territory of American Samoa (AS) is disproportionately vulnerable to SLR due to a high proportion of coastal development and limited land area (Nunn & Mimura 1997). However, Tutuila, which is the cultural and political center of AS, currently experiences an even higher rate of relative SLR due to the compounding effects of chronic geologic subsidence caused by viscoelastic relaxation following a disastrous 2009 earthquake. This subsidence, in addition to effects of global SLR, results in an effective SLR on Tutuila that is five times higher than the global average (Han *et al.* 2019). While the most noticeable effects of SLR typically manifest through surface flooding during acute or compounding events such as king tide or high wave events (Keener *et al.* 2021), a more insidious and chronic impact of SLR lies below, and occasionally above, the ground surface. Groundwater Inundation (GWI) has been identified around the world as an often-overlooked consequence of SLR (Rotzoll & Fletcher 2013; Masterson *et al.* 2014; Kane *et al.* 2015; Habel *et al.* 2017; Plane *et al.* 2019; Befus *et al.* 2020; Maliva 2021). This phenomenon not only causes inland flooding in areas disconnected from the sea, but can also raise the groundwater table, surreptitiously inundating buried infrastructure with salt water, which enhances corrosion and reduces lifespan through change in salinity and redox chemistry of the subsurface. Although there are few published case studies of GWI's effects on small tropical islands, its consequences when considered under future SLR projections suggest that GWI is likely to cause significant disruption to coastal and island communities in the future. For example, in the area of Waikiki on the Hawaiian Island of Oahu' Habel *et al.* (2017) used the MODFLOW model to determine that GWI is likely to put over $5 billion worth of real estate at risk of flooding with a SLR of 1 m. Knott *et al.* (2017) also used MODFLOW to determine that GWI reduced the service life of coastal roadway pavement in New Hampshire by 50–92%, and White *et al.* (2007) analyzed water table elevation data and found that GWI is the primary risk for the sustainability of drinking water supplies on small atolls such as Tarawa, Kiribati.

The water table in island aquifers typically manifests as a basal lens, with the top surface, or groundwater table, lying above mean sea level (MSL), and rising inland along a gradient toward higher terrain and typically higher recharge areas (Izuka *et al.* 2018). In high-recharge, volcanic-island aquifers the position and thickness of the freshwater lens is typically maintained in short-term equilibrium and primarily controlled by the rate of seaward flux. The magnitude of this flux, and thus the elevation of the lens, is ultimately driven by the interplay between the heterogeneous fabrics of formation permeability and groundwater recharge (Maliva 2021). Thus, as sea level rises in a flux-controlled system, the entire basal lens will generally rise an equivalent amount controlled by hydrostatic buoyancy (Werner & Simmons 2009; Bjerklie *et al.* 2012), as shown in Figure 1. In inland areas where the water table is already close to the ground surface this can manifest as flooding of basements and buried infrastructure, and in some cases, breakthrough surface flooding where groundwater seeps out and pools in depressions. This 'nuisance' flooding often occurs in low-lying areas disconnected from the ocean by higher seaward terrain. These effects are compounded not only by chronic SLR but also by acute alluvial events during heavy rains, where the unsaturated zone becomes so shallow that it cannot absorb rainfall, resulting in overland flow and widespread flooding (Habel *et al.* 2017; Rahimi *et al.* 2020). Therefore, it is critical that resource managers and policymakers not only consider the effects of bathtub-type surface flooding from SLR, but also recognize the additional challenges posed by GWI. Another major consequence from coastal GWI is the associated change in pore water salinity and/or redox conditions. These effects can drive increased corrosion or other unwanted chemical reactions that reduce the lifespan of certain materials, as well as the possibility of contaminant mobilization from legacy contamination locked up in soils (Suthersan 2001; Lu *et al.* 2018; Almheiri & Meguid 2019).

Water, power, and wastewater utilities in coastal regions are faced with significant climate adaptation challenges as they typically own and manage the majority of buried infrastructure. The American Samoa Power Authority (ASPA) is the sole provider of all three of the aforementioned services in AS and thus faces the unique challenges of managing a large number of critical assets in an isolated location that is especially vulnerable to climate change (Kumar & Taylor 2015; Han *et al.* 2019). While ASPA manages utilities across multiple islands in the territory, the economically and politically important Pago Pago Harbor area is one of the most vulnerable areas to GWI. The land fronting the harbor holds a large

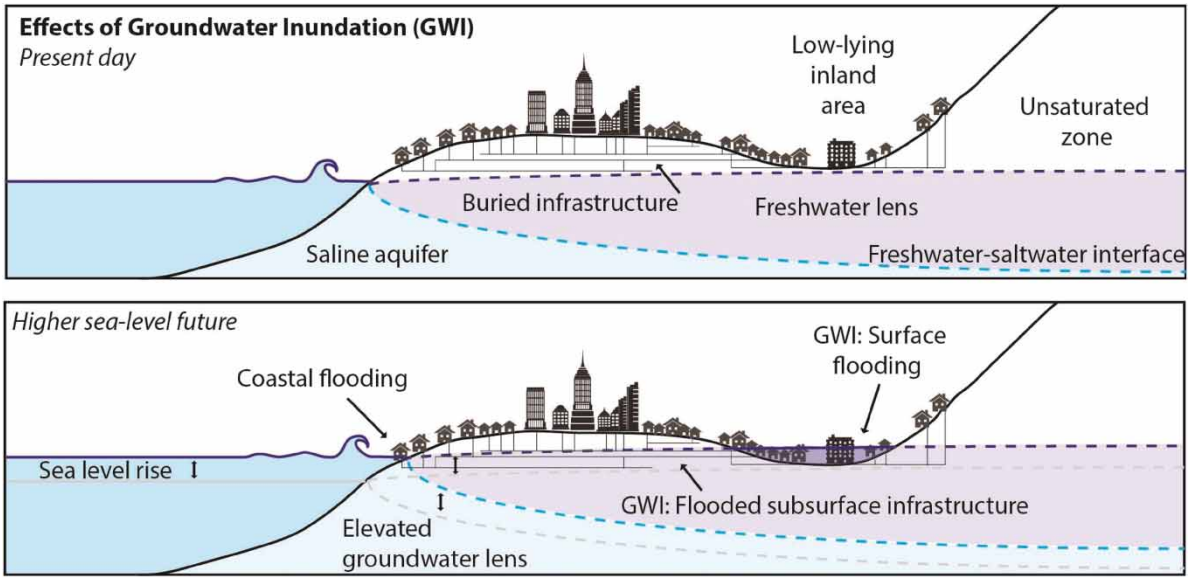

Figure 1 | Conceptual schematic of SLR-driven GWI and theoretical consequences in island settings. Top panel shows the built environment at the present-day sea level and the bottom panel indicates elevated sea level, water table rise, and the associated effects under SLR conditions.

concentration of infrastructure built on or under coastal plains that lie just above sea level. These assets include approximately 91 km of subsurface water lines, 42 km of below ground wastewater lines, 20 km of buried power lines, and 76 km of roads. In addition, there are eight sewer system lift stations, five water main booster stations, 2,400 individual mapped buildings, and 1,330 water meters located in the inner harbor area as well. Staff members at ASPA have already reported instances of inundated sewer lines and corroded manholes, thought to be a consequence of currently rising sea levels. There are also many other subsurface assets in AS that are vulnerable to negative effects of GWI for which no data currently exists, such as On-Site Disposal Systems and underground fuel storage tanks. In order for policymakers and utility providers to plan resiliently and to adapt to SLR, decision makers need accurate information regarding the projected locations and impacts of SLR. Without a clear understanding of where GWI vulnerabilities are most acute, the utility cannot prioritize limited resources and focus adaptation activities in the most critical locations. Mapping high priority areas will yield a more effective adaptation response and significant cost-savings in the long term.

This study aims to address these issues by pursuing the following objectives: (1) assessing the impact of GWI on surface and subsurface based infrastructure by modeling inundation at various levels of SLR, (2) assisting planners and utility managers in AS by mapping those areas that are most vulnerable to SLR driven GWI, which will aid in prioritization of adaptation activities, and (3) quantifying the individual effects of both SLR and projected changes in future rainfall on GWI impacts in Pago Harbor area.

2. METHODS

2.1. Study location

Tutuila is the main population center of the Territory of AS and is home to nearly 56,000 permanent residents. Located near 14° S and 170° W and within the South Pacific Convergence Zone, the climate is hot, humid, and has prevalent year-round rainfall, up to 6,000 mm/year along the mountain tops. The rainier season lasts from October to May, with the rest of the year experiencing less but still significant rainfall (NWS 2000). The 142-km^2 island is composed of the remnant core of a group of eroded basaltic shield volcanoes (Stearns 1944) and due to the heavy and prevalent rainfall, the landscape has been dissected into steep ridges and valleys. This has concentrated human development on thin coastal plains formed by alluvium and marine deposits during recent sea level high-stands (Stearns 1944; Grossman *et al.* 1998; Blanchon *et al.* 2009). The Pago Pago Harbor area (Figure 2) lies within an ancient collapsed caldera and is documented as one of the best natural harborages in all of the South Pacific. The Harbor is home to a number of villages including the Village of Fagatogo, which is the seat of AS's territorial government, and Atuu Village, the home of the island's only industry and largest private employer, the StarKist

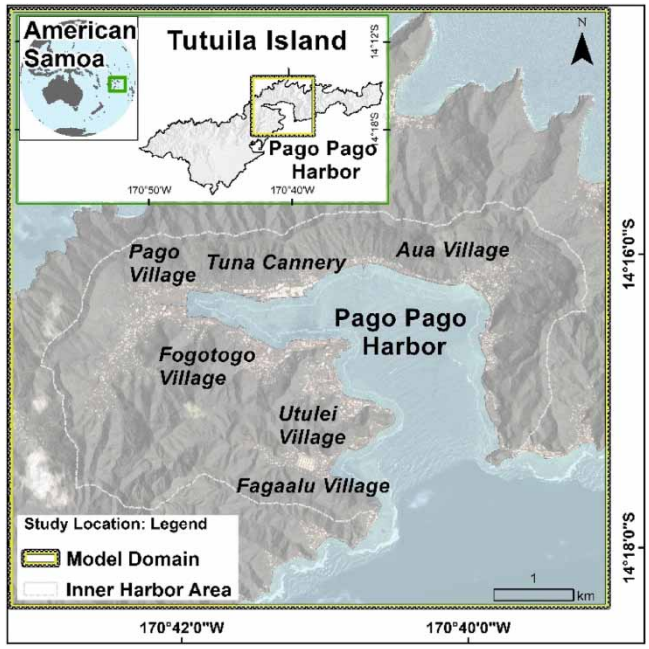

Figure 2 | Regional and study location map showing the general location of AS (approximately 7,600 km SW of the USA and 4,000 km E of Australia), in the smallest inset map, Tutuila Island and the location of Pago Harbor within the green box and second inset map, and Pago Harbor and the groundwater model domain boundary within the main map as delineated by the yellow and black border. The watershed boundary of Pago Harbor drainages is shown as a dashed gray line and selected villages are labeled.

Tuna Cannery. Overall, the extremely steep terrain and the concentration of government and industrial facilities has resulted in a large part of the territory's built assets being concentrated on the low-lying coastal plains inside of the harbor, which are highly vulnerable to impacts of SLR. Additionally, some villages in the harbor area are said to be underlain by fill composed of bulky waste from the era of US Navy occupation. Contaminants have already been found in coastal sediments offshore of some of these villages (Whitall & Holst 2015) and GWI only produces additional risk that, if present, contaminants may be mobilized from these land-filled areas.

In order to assess the frequency and future risk of subsurface flooding on infrastructure, a MODFLOW based groundwater model was developed for Tutuila's Pago Harbor Region and included SLR data produced by the National Oceanic and Atmospheric Administration (NOAA) Office of Coastal Management and presented on NOAA's national SLR viewer (OCM 2016) to modify the base ocean elevation and the coastline position for multiple future climate and SLR scenarios. The range of possible SLR levels predicted by NOAA in the year 2090 was considered. Although the timing of when a given SLR value will occur remains uncertain, presenting a reasonable range of probable SLR heights ultimately gives present-day managers an understanding of risks that encompass the varying range of emissions trajectories possible during the next seven decades. Because climate drivers, such as precipitation, are also projected to be different in the future, our future scenarios also incorporated a dynamically downscaled groundwater recharge coverage of a Representative Concentration Pathway (RCP) 4.5 emissions pathway developed previously by Shuler *et al.* (2021) for the period 2080–2100 using the only available downscaled climate projections from Wang & Zhang (2016). The RCP4.5 pathway was selected as it represents the most extreme increase in precipitation, about 14% island-wide, of the available scenarios. Modeled water table elevations for present and future scenarios were then used to assess where subsurface and surface-based infrastructure would be permanently submerged below the water table, or affected by nuisance flooding, respectively.

2.2. Groundwater modeling methods

2.2.1. Existing modeling framework and input data

The modeling framework used for this project was followed from the collaborative modeling framework developed by Shuler & Mariner (2020). Specifically, the model used for this study is derivative of three existing products: (1) a downscaled climate

model produced by Wang & Zhang (2016) that was used as input to (2) a SWB-based water-budget model produced by Shuler (2019), which provided the present and future climate informed recharge coverages that were used as input to (3) an island-wide numerical groundwater model described in Shuler & Mariner (2020). Specific details about the aforementioned products are described in the respective publications and are omitted here for brevity. The modeling framework was produced in a reproducible open-source manner by employing the Python package FloPy to manage model development and to document all code-based model scripts via Jupiter Notebooks (Kluyver *et al.* 2016) in an open-source repository on GitHub (Shuler 2022). MODFLOW has been previously proven to be an effective model for simulation of coastal GWI in high-island settings (Masterson *et al.* 2014; Habel *et al.* 2017), and a newer study by Habel *et al.* (2019) suggests that using more computationally or time intensive density dependent models such as SEAWAT is not necessary to accurately simulate local groundwater gradients for successful GWI simulation.

2.2.2. The GWI model

For this study, a 7.5 × 7.5 km region surrounding the Pago Pago Harbor was delineated as the single-layer model domain (Figure 3), and it was divided into 2.25 million model cells to achieve a 5-m cell resolution. Top elevations were assigned from a 1-m resolution digital elevation model (DEM) (OCM 2012) and the bottom elevation was held constant at a depth of 500 m below MSL. The shoreline was assigned a specified head boundary at 0 MSL for the base scenario, and terrestrial boundaries were assigned a specified head equivalent to the head level taken from the island-wide model detailed in Shuler & Mariner (2020). Shoreline position, based on NOAA SLR scenarios (OCM 2016), and sea level-based specified heads were modified accordingly for each of the three SLR scenarios. Oceanic areas outside of the coastal specified head boundaries were assigned an inactive status. Streams were simulated as drains and major channels were obtained from the National Hydraulic Dataset (USGS 2018). Pump rates for active wells in the model domain were obtained from ASPA and were set at their average extraction rates calculated between 2005 and 2017, representing the period of highest-quality available data. A total of 27 water level observations at wells detailed in Shuler & Mariner (2020) were used for model calibration. Recharge for both present-day and future climate RCP4.5 scenarios were clipped from the island-wide high-resolution recharge coverages of Tutuila produced by Shuler *et al.* (2021). Spatially distributed horizontal hydraulic conductivity (hK) values were obtained through calibration using a zone-based approach based on the 11 geologic units within the Pago Harbor area as defined by Stearns (1944). Note that the model was a one-layer model; thus, it does not include values for vertical hydraulic conductivity or anisotropy.

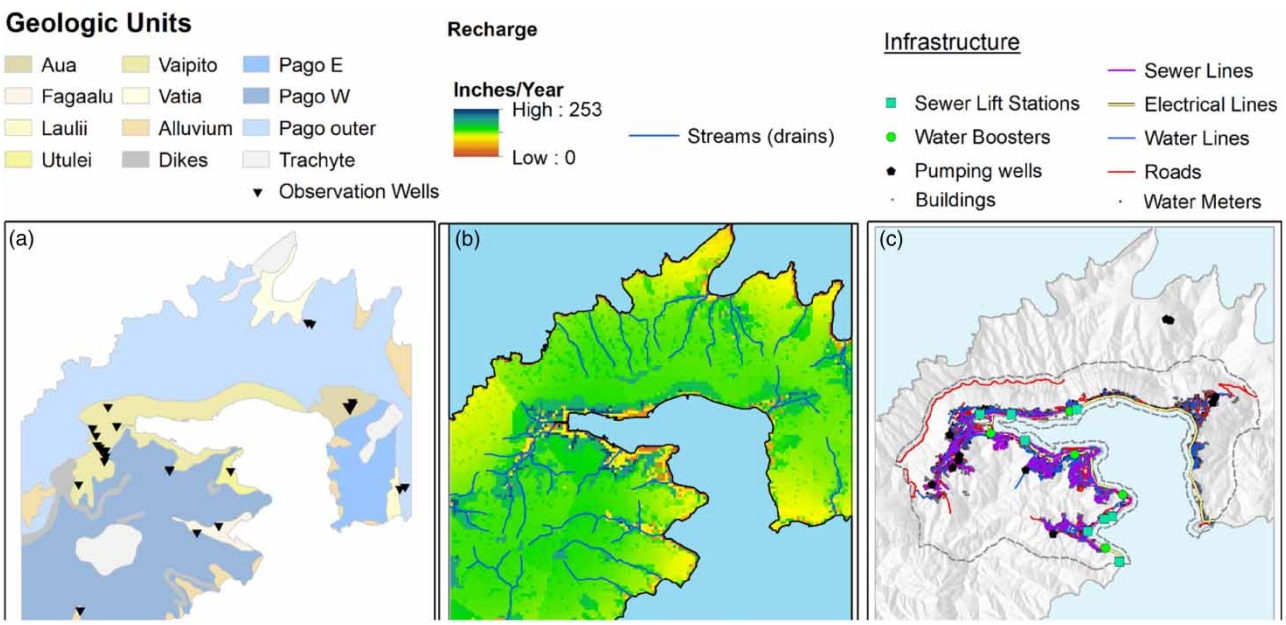

Figure 3 | Maps showing the spatial distribution of model parameters. (a) Hydrologic conductivity (hK). (b) Average annual groundwater recharge (in./year) and stream/model drain locations. (c) Buried and surface-based infrastructure locations in the Pago Pago Harbor area.

The FloPy model was run using MODFLOW 2005 and the resulting water table surface was used to assess the depth to groundwater by geospatially subtracting the land surface height at each cell. This provided a spatially distributed estimate of the depth to groundwater throughout the entire model domain.

2.3. Subsurface and surface-based infrastructure data

Stakeholder involvement was a key element and many of the critical input datasets were provided by ASPA, including water level observations, well extraction rates, and infrastructure locations. Two-dimensional as-built drawings of water, sewer, and buried electrical infrastructure (items 1–6 below) were obtained directly from ASPA as CAD or GIS-shapefiles. Shapefiles of roads and buildings were obtained from the AS Department of Commerce GIS-Portal (ASDOC 2015). Infrastructure considered in this assessment included:

1. Transmission and Distribution water mains
2. Sewer lines
3. Water system booster stations
4. Sewer system lift stations
5. Customer water meters
6. Buried electrical lines
7. Roadways
8. Buildings

Since the depth of buried assets is variable and none of the available data files contained vertical dimensionality, the average depth for all subsurface infrastructure was assumed to be 1 m. This estimate is considered to be conservative as staff members at ASPA have confirmed that many of their buried pipes are located even deeper, especially when placed under roads or other areas with vehicle traffic. Subsurface infrastructure included water, sewer, and buried electrical lines as well as sewer lift stations since most lift station components are located below grade. Surface-based infrastructure included water boosters, roads, buildings, and customer water meters. Roads and buildings shapefiles circa 2009 were obtained from the AS geographic information system (GIS) users' group. All shapefiles and as-builts were clipped to their extent within the inner harbor area shown on Figure 3. While the model boundary does include some outer villages on the north and south shores, infrastructure in these areas was not included due to boundary condition effects. To determine where infrastructure was flooded, all cells within the depth to water coverage(s) with a value less than 1 m for subsurface infrastructure and less than 0 m for surface infrastructure were aggregated into a single 'flooded area' shapefile, and geospatial locations of infrastructure were intersected with the flooded areas. This method was reproduced for each SLR and climate change scenario to calculate the total length or number of each infrastructure asset type that were modeled as flooded for each scenario.

2.4. SLR and future climate scenarios

Three different levels of SLR were selected for use in the model based on projections provided by the 2017 NOAA Sea level Viewer: 0.6 m (≈2 ft) SLR, 1.5 m (≈5 ft) SLR, and 2.4 (≈8 ft) m SLR. These sea levels are representative of different possible SLR projections at different times. Climate projections are often produced at the end-of-century resolution and managers often plan for these long-term timelines; thus, the year 2090 was selected as a key point in our assessment. Specifically in the year 2090, 2.4 m SLR is considered by the NOAA SLR viewer to be the 'extreme' scenario, 1.5 m SLR is the 'intermediate high' scenario, and 0.6 m SLR is the 'intermediate low' scenario (OCM 2016). These projected sea levels also correspond to other potentially useful points of reference; specifically, 1.5 m SLR is the 'extreme' scenario in the year 2070, and 0.6 m SLR is the 'extreme' scenario in the year 2040. The year 2040 is currently well within the engineering lifespan of most surface and subsurface infrastructure components, making this point of reference useful for informing present-day equipment procurement decisions. The year 2090 is also likely to have a different climate and thus a different groundwater recharge distribution than the present day. To account for this, the only available future climate informed groundwater recharge coverage was used (Shuler *et al.* 2021) as an input to the MODFLOW model. This future recharge coverage was derived from the only available downscaled climate model for AS (Wang & Zhang 2016), based on the RCP4.5 emissions projection for the period 2080 to 2100, which was selected as it represented the largest rainfall anomaly of Wang and Zhang's modeled emissions scenarios.

2.5. Model calibration and sensitivity testing

By using the FloPy package, the MODFLOW executable and all processing of model inputs could be run directly from a single Python interface. This allows the model to be easily wrapped into a loop function and parameters to be varied to assess performance under different controlled parameterizations for both calibration and sensitivity testing. Model calibration was performed for the most uncertain model parameter, of horizontal hydraulic conductivity (hK). Spatially distributed hK values were varied using a zone-based approach with a unique hK parameter for each of the 11 geologic units in the model. The model cost function was defined as the root-mean square error (RMSE) between the set of computed and observed water levels (Figure 4) at 27 observation points (groundwater wells) located within the model domain and described in Shuler & Mariner (2020). The Python Package Scipy (https://www.scipy.org/) contains a scalar optimization function 'scipy.optimize.minimize' that was used iteratively to optimize the cost function and determine the best fitting hK values. Ultimately calibration resulted in an RMSE of 2.6 m, which was deemed to be acceptable once systematic bias was not observable and subsequent calibration iterations yielded no significant improvement in RMSE.

The model wrapper function was also applied in a sensitivity test of the model response to independent perturbations of each of the hK values and other key parameters including stream conductance, well pumping rates, and recharge rates. The final objective value, represented by the total length of flooded subsurface water and sewer lines, was calculated for each sensitivity test case and the resulting percent difference in this value between each test case and the base case scenario (no perturbations) was recorded. While it is not possible to directly quantify model uncertainty due to the iterative and non-linear nature of the model, sensitivity testing not only shows which parameters are most important, but also allows for an understanding of how much of the model uncertainty is derived from each parameter. Results of sensitivity tests are presented in Section 3.2.

3. RESULTS

Assessing impacts of GWI on surface and subsurface based infrastructure: For the present-day calibrated base case scenario, the model indicated that less than 1% of surface infrastructure, and less than 4% of subsurface infrastructure, is currently affected by GWI. This is a reasonable figure according to ASPA operations staff, and helps to validate the model's accuracy. For the different future SLR scenarios, GWI effects grade toward the most extreme case, where in the 2.4 m SLR scenario,

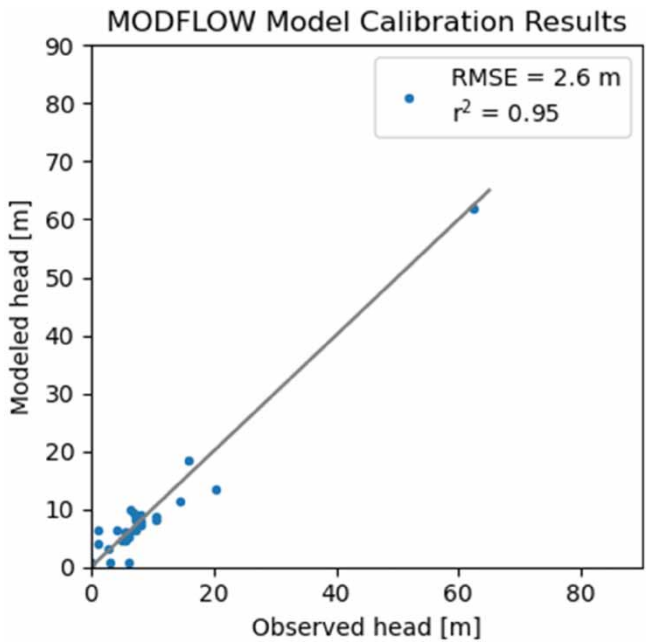

Figure 4 | The 1:1 plot of MODFLOW model calibration results showing observed (*X* axis) and model-computed (*Y* axis) water levels (heads) at groundwater wells within the model domain as calculated using the present-day MODFLOW model. The calibrated model had an RMSE of 2.6 m and an r^2 of 0.95.

which also includes the 2090 RCP4.5 climate regime, the model calculates that 30–90% of subsurface infrastructure, and 10–30% of surface infrastructure, may be affected by GWI or surface flooding, respectively. In this worst-case scenario, the model calculated that 21.4 km of roads would be flooded, 13 km of sewer lines, 7 of the 8 sewer lift stations flooded at their bases, 18.7 km of buried electrical lines, and 37.6 km of inundated water lines. For context, replacing 37.6 km of water lines would require approximately 6,200 individual 20-foot-long pipes, which if assuming each had a 12-inch outer diameter, would require 85 semi-truck loads to transport. The model assessed GWI impacts on eight individual infrastructure types, across a large region. While the exact locations of GWI impacts on each of these assets can be seen by plotting the associated shapefiles in the project repository (https://github.com/cshuler/Pago_GWI_Modeling), a higher-level synthesis is useful for managers and policy makers. This is shown in Table 1, which shows the percentage of the total number of point assets or the total length of linear assets affected by GWI for each scenario.

Mapping areas most vulnerable to GWI: In all scenarios, the majority of impacted infrastructure features are primarily located in those areas of heavy development built upon the relatively low-elevation coastal plains at the valley mouths. These areas include: Fogotogo Village, Utulei Village, Pago Village, and Aua Village. Figure 5 shows the depth to groundwater in the inner harbor area for the present day and each of the three SLR scenarios, whereas all areas in blue are flooded at the surface, and areas in green have less than 1 m of unsaturated space, resulting in assumed flooding of subsurface infrastructure. Areas in orange and red indicate where the unsaturated space is less than 2 and 3 m, respectively, which could be an issue for deeper infrastructure.

Quantifying the impacts of SLR vs. future climate on GWI: While the future simulations presented here included both future SLR and future downscaled recharge projections, isolated scenarios with only one of each of these drivers were also run to assess the contribution of each driver on the final results. For summarization, calculating the average cell-by-cell increase between the future-climate coverage (RCP4.5) and the base case climate coverage indicated that the future climate was on average simulated to be 12 $\pm$ 0.04% wetter than the base case. However, this 12% increase only translated into increases of 7.2, 1.4, and 0.42% of inundated subsurface water and sewer lines for the 0.6, 1.5 and 2.4 m SLR scenarios, respectively. This result suggests that the forcing from SLR, especially at the higher SLR levels, is the primary driver of increased nearshore groundwater levels rather than the increase in recharge at the magnitudes predicted by the Wang & Zhang (2016) projections.

3.1. Assessment of model performance: present-day validation

In order to assess the model performance under present-day conditions, the depth to water surface was carefully examined. Areas where the model calculated present-day surface flooding were compared to locations where standing open water is known to exist in the present day across the landscape (streams, canals, and wetlands), as observed during field visits and confirmed by aerial orthoimagery. Overall, the model did an acceptable job of predicting locations where standing water exists in hydrologic

Table 1 | Length or number of flooded infrastructure assets, both surface and subsurface, in the Pago Pago Harbor under different scenarios of SLR and future climate

	Total assets (km or #)	Present day (% flooded)	0.6 m SLR 2090 climate (% flooded)	1.5 m SLR 2090 climate (% flooded)	2.4 m SLR 2090 climate (% flooded)
Subsurface					
Water lines	91.2 km	3.8	12.3	30.4	41.1
Sewer lines	42.3 km	3.5	12.1	27	32.5
Electrical lines	20.5 km	10.8	29.4	71.1	91.1
Sewer lift stations	8	0	0	50	87.5
Surface					
Water meters	1,329	0.1	0.2	2.1	10.7
Water line boosters	5	0	0	20	20
Roads	76.8 km	0.1	0.5	4.7	28
Buildings	2,398	0	0.1	3.2	13.6

The 'Total assets' column gives lengths of linear assets in metres (m) and number of flooded point assets. Other columns show the percentage of the total length or numbers that are simulated to be flooded in the given scenario.

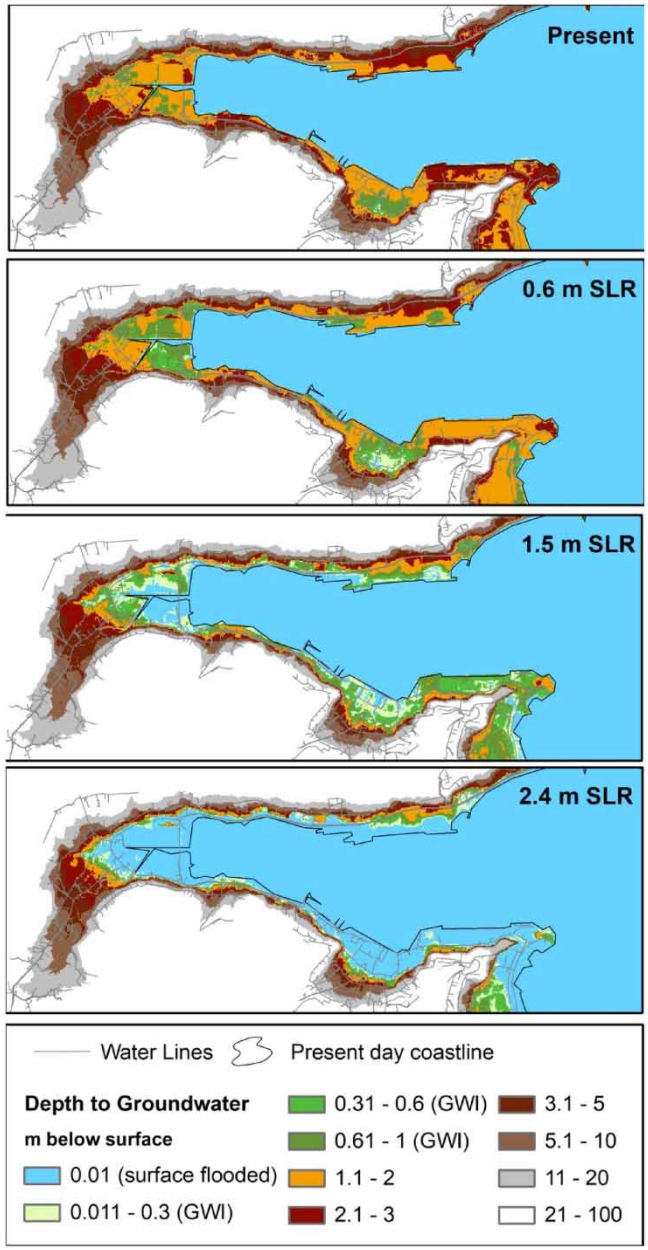

Figure 5 | Model calculated depth to groundwater in the inner harbor area for the present day and the three SLR scenarios. Colors indicate depth of groundwater below the land surface with blue indicating surface flooding. Green shades indicate where the groundwater levels are modeled to be less than 1 m below land surface. To show infrastructure impacts, water lines are overlaid on the figure as gray lines. Other infrastructure layers are omitted for clarity.

equilibrium with the basal water table (Figure 6). While this validation was limited to a qualitative assessment, it nonetheless provides some additional confidence in the model's ability to accurately predict the water table elevation.

3.2. Assessment of model performance: sensitivity test results

The sensitivity of the model to each of its input parameters was assessed through an analysis that compared the extent of GWI impacts between different model runs each with an isolated perturbation in input parameter values. Four separate runs were conducted for each of the 15 tested input parameters, with each being individually decreased by a factor of 2× and 4×, and also increased by a factor of 2× and 4×. The reference output value used to quantify the comparison of each run was a domain-wide calculation of the total length of flooded subsurface water and sewer lines. Results indicated that the model

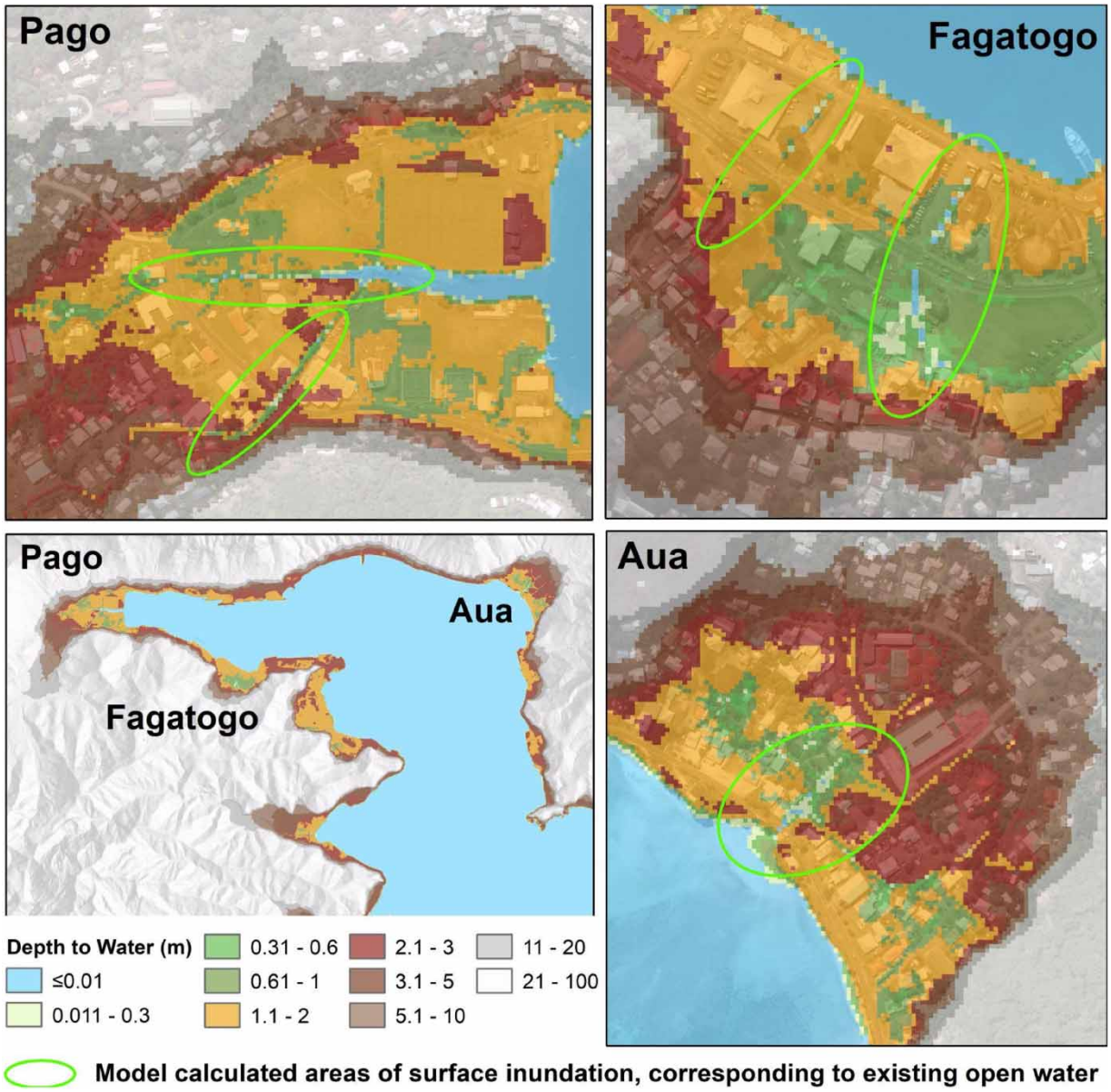

Figure 6 | Comparison between present-day model calculated areas of surface flooding with known open-water features (streams, canals, and wetlands) across the landscape.

was most sensitive to hK values, and specifically those in the alluvial geologic units that underlie villages containing a significant amount of development (Table 2). These were namely Pago Village (Vaipito unit) and Utulei Village (Utulei Unit). As expected, increases in hK reduced the amount and extent of GWI, and decreases in hK resulted in increases in GWI related flooding overall. Additionally, the model was quite sensitive to recharge and well pumping rates, which are both known to be major controls on groundwater heads.

4. DISCUSSION

4.1. Management applications

The most direct application of this study is by managers and decision makers at utilities or agencies in AS who are faced daily with needing to make site-specific procurement and planning decisions for the future. The maps produced for this project have already been deemed 'very useful' to these ends by the executive director at ASPA. Since the catastrophic 2009

Table 2 | Sensitivity test results expressed as the percentage difference in the reference value between the test case and the base case scenarios for perturbations of individual parameters at 25, 50, 200, and 400% from the base case scenario

Parameters	Percent change in reference value – 25% multiplier	Percent change in reference value – 50% multiplier	Percent change in reference value – 200% multiplier	Percent change in reference value – 400% multiplier
hK-Aua (0.9 m/d)	8.9%	4.0%	−2.3%	−4.3%
hK-Fagaalu (24 m/d)	11.6%	3.9%	−2.5%	−4.9%
hK-Laulii (0.9 m/d)	0.0%	0.0%	0.0%	0.0%
hK-Utulei (0.5 m/d)	68.3%	35.4%	−7.6%	−9.2%
hK-Vaipito (1.5 m/d)	124.5%	61.6%	−67.3%	−73.0%
hK-Vatia (0.4 m/d)	0.1%	0.0%	−0.2%	−0.4%
hK-minor (5.1 m/d)	1.7%	0.4%	−0.7%	−1.1%
hK-Dikes (0.002 m/d)	2.2%	−0.4%	0.0%	0.0%
hK-Pago-Inner-East (1.6 m/d)	−0.8%	−0.1%	−0.3%	−1.1%
hK-Pago-Inner-West (0.4 m/d)	11.1%	4.6%	5.3%	6.0%
hK-Pago-Outer (0.43 m/d)	6.0%	3.3%	−6.6%	−15.3%
hK-Trachyte (0.0004 m/d)	−0.3%	0.0%	0.0%	−0.2%
Stream Conductance (35 m/d)	6.3%	2.2%	−1.4%	−2.1%
Well pump rates (variable)	11.1%	6.7%	−20.1%	−68.7%
Recharge (variable)	−85.5%	−82.0%	138.4%	312.9%

The reference value was defined as the modeled percent change in the total length of flooded subsurface water and sewer lines through the whole model domain. Positive values indicate more flooded lines and negative values indicate less. Values of hK refer to the hydraulic conductivity in m/d of the area associated with each of the conductivity zones defined in the MODFLOW model (e.g. the Aua or Fagaalu zone). Note that all parameters are scalar values except for well pump rates and recharge, which are a set of point values and a gridded raster, respectively. These were all modified at once by the multiplier value for each test scenario.

earthquake and Tutuila's acceleration in relative SLR (Han *et al.* 2019), utility managers in AS are already responding to the impacts of SLR. Workers at ASPA have noted instances of manholes corroding and heavy inflows and infiltration in sewer lines in low-lying areas. Our modeling suggests these problems will only be exacerbated by continued SLR and GWI, particularly in the lowest-lying areas of Pago Harbor. Another impact that is likely already occurring, but has not necessarily been attributed to GWI, is an increased depth of floodwaters in low-lying areas during rain events. GWI has been shown globally to be a major factor in exacerbating flooding from alluvial sources and heavy rainfall (Habel *et al.* 2017; Maliva 2021). All of the main population centers in the Pago Harbor area are located on alluvial plains at the base of mountain streams. Increases in the permanent soil saturation level underlying these plains reduces the infiltration capacity of these low-lying areas and can result in increased flooding or ponding when even smaller rain events occur.

In general, the presence of low-lying, inland sink areas identified by this work provides a clear caution against relying entirely on gray infrastructure such as seawalls as an adaptation measure. Even if a seawall or levee can hold back encroaching ocean waters on the surface, these structures will not be able to mitigate flooding or continuously saturated soil in areas that are hydrologically connected to the sea. In AS, seawalls have historically been the primary response to coastal erosion and rising seas. The issues noted herein only add to the many other commonly known negative side-effects of seawalls (Nunn *et al.* 2021), thereby reinforcing the idea that more advanced 'green-engineered' solutions or possibly even managed retreat from low-lying areas may be a more appropriate adaptation strategy in the long term.

4.2. Geologic controls on vulnerability to SLR and GWI

There are many other islands throughout the world's oceans that are already or are very likely to experience similar consequences of GWI as Tutuila. However, each island hosts a unique set of vulnerabilities, partially controlled by development patterns, but also controlled by their geologic setting. To better understand the drivers of GWI vulnerability across different

islands, this section examines the geology that controls the impacts and severity of GWI. Tutuila serves as a unique and interesting example, because although the Pago Harbor area is highly vulnerable to GWI, other parts of Tutuila are less vulnerable because of the island's diverse and varied geologic history. The southwestern part of the island, the Tafuna-Leone Plain (T-L Plain), is geologically younger and is characterized by an extensive lava delta fronted mostly by sea cliffs. Almost all of the T-L Plain is at or above 5 m in elevation, making SLR mostly inconsequential to the built environment. This shows the level of control that geologic processes have on vulnerability to SLR in volcanic islands; and how better understanding local geologic histories can be informative in region-wide adaptation planning efforts. Specifically, on Tutuila and other islands, two main factors control the conditions that lead to high vulnerability to GWI: (1) substrate age and (2) coastal geometry at the time of the last sea level high-stands. An island's age is one of the primary variables controlling the amount of developable land on an island, due to the effects of erosion and weathering that incise islands into a series of steep valleys and craggy peaks that preclude development. Generally, older islands are more eroded, and thus contain less developable land, which results in consolidation of development into the few flat areas, which are often thin coastal plains. Other examples of this type of terrain include much of the islands of Oahu (2.2–3.4 MYA) and Bora Bora (3.1–3.5 MYA). The eastern portion of Tutuila is included in this group because although relatively younger at 1.5 MYA, Tutuila's location within the South Pacific convergence zone creates very high rainfall rates that have enhanced erosion and weathering. Contrastingly, the Tafuna Leone Plain erupted within the last 10,000–20,000 years (Addison & Asaua 2006) and displays a flatter dome shaped geography characteristic of young shield volcanoes. Other young volcanic islands that share this terrain include Hawaii's Big Island (<0.5 MYA), Rapa Nui (<0.7 MYA), and Isla Isabella in the Galapagos (<0.7 MYA). These younger shields all generally have less eroded features, which make development away from the coast more common and cost-effective. Also, a lack of well-developed coral reefs, again due to younger geologic age, focuses wave energy directly on the coastline, thereby leading to development of sea cliffs that allow coastal development to be elevated above the sea, thereby simplifying adaptation to SLR.

Another geologic factor relating to an island's level of vulnerability to GWI is the coastal geometry at the time of the last sea level high-stands, which directly controls the prevalence of low-elevation coastal plains. These plains were formed in shallow depositional environments during major interglacial periods. Isotopic and marine records show that the Last Interglacial (130,000–120,000 years ago) sea level high-stand that ranged between 1–3 m created extensive coastal plains in the Hawaiian Islands (Ku *et al.* 1974; Szabo *et al.* 1994), which also manifest throughout the Northern and Southern Pacific (Muhs *et al.* 1994; Nunn & Mimura 1997). For example, Waikiki, the tourism-driven economic engine of Hawaii, is built entirely on one of these low-lying coastal plains, and in many places the ground sits around 2 m above MSL. Other developed areas on Oahu, such as the Eva Plain, were also deposited during these sea level high-stands, which caused shallow depositional environments to form, often behind barrier or fringing reefs. Thus, the presence of shallow lagoons and nearshore barrier or fringing reefs during the last interglacial high-stands is a major controlling factor in coastal plain development. Because these flat, nearshore areas are now desirable for residential and business development, and are easy to build upon, many of them have been extensively developed, creating a situation where some of the Pacific Island's most valuable real estate is situated in areas that were originally, and will likely soon again be, in a shallow depositional environment.

4.3. Assumptions, limitations, and uncertainties

With any modeling study it is important to clearly understand the specific limitations and the conditions required to make use of results and to avoid overinterpretation. For this work, a key assumption relies on the accuracy of the modeled water table elevations, the DEM surface elevations, and the infrastructure locations relative to each other and to a common sea level-based datum. Lidar data for the 1 m DEM used in this study was originally collected in 2012 and represents accurate elevations only during a snapshot in time. It is well known that ongoing geologic subsidence is and has been changing AS's observed sea level baseline relative to the global datum; therefore, sea levels presented here should not be considered to be accurate in terms of absolute elevations. However, assuming that the subsidence induced land motion is primarily vertical in direction, the relative elevation differences between the base case and future scenarios used in this work should still remain accurate, as both the MODFLOW model and the geospatial analysis used the same 1 m DEM as their base datum.

The majority of uncertainty in the outputs likely arises from the MODFLOW calculated water table elevations due to the large number of difficult to constrain inputs used in the model. The model is limited by its most poorly constrained parameter, which, as shown by results of sensitivity testing, was the subsurface hK. Although the best available water level data was used to calibrate the model hK values, difficulty in constraining this parameter typically contributes the most to model uncertainties. Although this uncertainty cannot be propagated through the model (because it is run iteratively), the sensitivity testing

revealed that uncertainties in the hK values of the most highly sensitive units, specifically Vaipito and Utulei, may be the most important components in the final synthesis of results. It should also be pointed out that the depth of infrastructure was assumed. Unfortunately, the complete lack of depth data not only precludes accurate vertical placement of features but also makes it impossible to assess the uncertainty associated with using a single depth. While a depth of 1 m was determined to be the best available assumption based on discussion with operations and field staff at ASPA, it is nonetheless a significant generalization. Finally, it should be noted that the horizontal accuracy of most utility-grade as-builts is subject to errors, as their locations are often poorly documented in records that are often quite old. Indeed, utility companies typically have to perform geophysical utility locates to avoid hitting buried pipes and lines while digging. Nonetheless, these datasets represent the best available infrastructure data, and with the groundwater model cell size of 5 m, it is likely that inaccuracies in the infrastructure locations do not significantly bias results.

Other notable assumptions include ignoring the dual-density effects of seawater, leading to our decision not to use more computationally expensive models such as SEAWAT or SUTRA that consider these effects. This decision was based on the findings of Habel *et al.* (2019), which used an even simpler approach and determined that a more complex modeling framework would not necessarily yield more accurate results. Although seawater recirculation will cause variation in water table elevations very near the coast, these are likely to be negligible at the region-wide scale where hydrodynamic lift in the water table will likely make up the bulk of effects of SLR on the aquifer. Additionally, because there are no dedicated monitoring wells in AS, water levels used for calibration were taken from shut off pumping wells as described in Shuler & Mariner (2020). The predominant assumptions in using this approach are that (1) the well recovery tests yielded fully recovered water levels, and (2) the effects of nearby pumping wells did not extend to the measurement point when the recovery tests were taking place. Therefore, the model was calibrated to a hypothetical state with no aquifer pumping. While this could lead to some inconsistencies if extraction wells were added into the model, the lack of other observation data precluded the use of a better method. Additionally, it was determined that the limited spatial extent of well drawdown cones, the variability of pumping rates, and the likely possibility of existing wells going offline and new wells being drilled by 2090 precluded the inclusion of well extraction in the model scenarios.

5. CONCLUSIONS

By intersecting a numerical groundwater model, future climate and SLR projections, and as-built locations of buried and surface-based infrastructure, this work produced estimates of the 'hidden' impacts of SLR, manifested as GWI in Pago Pago Harbor, home of the capital of AS. The primary future climate forcings applied in the model framework were NOAA's SLR projections at 0.6, 1.5, and 2.4 m, which bracket the uncertainty range for SLR in the region by the end of the century. Future climate forcing in the form of a modified groundwater recharge coverage was also included in our future modeled projections. Under these three SLR scenarios, the model predicted inundation of an average of 13, 44, and 63% of all buried infrastructure considered in the model, respectively. At higher SLR levels direct surface flooding will also be widespread, and our model predicts in the worst case of 2.4 m SLR that 18% of present-day surface-based infrastructure will be permanently flooded. Vulnerability to GWI impacts was greatest in areas of heavy development built upon the relatively low-elevation coastal plains at the valley mouths including Fogotogo Utulei Pago and Aua Villages. At 0.6 m of SLR, the projected increases in rainfall contributed somewhat to increases in GWI, but at higher levels of SLR impacts of GWI were almost completely due to SLR, and climate forcing was found to be an insignificant factor.

Overall, the results of this study have farther reaching implications beyond AS that can provide insight to other island communities likely to be facing similar challenges. Many island societies have historically been based around a paradigm of static sea levels, and it is clear that planning decisions can no longer be made within that framework. The maps produced by this model are by no means an exact prediction of the future, but they can assist managers in identifying the lowest-lying areas and zones where infrastructure intersects and may be vulnerable to both surface induced and groundwater caused SLR impacts. Recommendations based on the results of this work could include locating new utilities in areas not prone to GWI, or if existing utilities are already located in these areas, replacement timelines should consider reduction of service life and replacement with corrosion- and water-resistant materials. Further research to better document the actual depths of subsurface infrastructure would be useful to refine the estimates of impact presented herein. The conditions modeled in this study are often overlooked by or unknown to managers, and it is hoped this work helps to contextualize the risks associated with

SLR in these types of terrains, and helps to prioritize where adaptation actions can have the greatest surface and subsurface benefit.

ACKNOWLEDGEMENTS

The models and inundation maps were co-produced with operations and engineering staff at ASPA, including Katrina Mariner, Wei Hua-Hsien, Will Spitzenberg, and Danielle Mauga, and the author is thankful to ASPA's leadership, especially Executive Director Wallon Young for the agency's support and openness to encouraging and applying the best available science. This work would not have been possible without the critical mentorship of modelers at the USGS Pacific Islands Water Science Center, including Scot Izuka and Kolja Rotzoll, as well as my mentors at the University of Hawaii, including Aly El-Kadi, Henrietta Dulai, and Craig Glenn. All shapefiles, data, model files, and maps are open-source and are available on GitHub (https://github.com/cshuler/Pago_GWI_Modeling). Funding for this work was provided by NOAA's Climate Program Office through the Pacific Research on Island Solutions for Adaptation (RISA) program, Grant number: NOAA-OAR – CPO – 2015 – 2004099.

DATA AVAILABILITY STATEMENT

All relevant data are available from an online repository or repositories: https://github.com/cshuler/Pago_Samoa_GWI.

CONFLICT OF INTEREST

The authors declare there is no conflict.

REFERENCES

Addison, D. J. & Asaua, T. 2006 100 new dates from Tutuila and Manu'a: Additional data addressing chronological issues in Samoan prehistory. *Journal of Samoan History* **2** (95e), 119.

Almheiri, Z. & Meguid, M. 2019 Buried Infrastructure in Saline Soils: A Review. In: *Proceedings of the Conference: Canadian Society for Civil Engineering*, Laval, QC, Canada, pp. 12–15.

ASDOC – American Samoa Department of Commerce 2015 *American Samoa CMSP Data Portal*. Available from: https://www.arcgis.com/home/item.html?id=7db19f0ac94e4f97abc10711e7f540bc (Accessed Oct 2015).

Befus, K. M., Barnard, P. L., Hoover, D. J., Hart, J. F. & Voss, C. I. 2020 Increasing threat of coastal groundwater hazards from sea-level rise in California. *Nature Climate Change* **10** (10), 946–952.

Bjerklie, D. M., Mullaney, J. R., Stone, J. R., Skinner, B. J. & Ramlow, M. A. 2012 *Preliminary Investigation of the Effects of Sea-Level Rise on Groundwater Levels in New Haven, Connecticut*. USGS OFR 2012–1025 (USGS). Available from: https://pubs.usgs.gov/of/2012/1025/pdf/ofr2012-1025_report_508.pdf.

Blanchon, P., Eisenhauer, A., Fietzke, J. & Liebetrau, V. 2009 Rapid sea-level rise and reef back-stepping at the close of the last interglacial highstand. *Nature* **458** (7240), 881–884.

Grossman, E. E., Fletcher III, C. H. & Richmond, B. M. 1998 The Holocene sea-level highstand in the equatorial Pacific: Analysis of the insular paleosea-level database. *Coral Reefs* **17** (3), 309–327.

Habel, S., Fletcher, C. H., Rotzoll, K. & El-Kadi, A. I. 2017 Development of a model to simulate groundwater inundation induced by sea-level rise and high tides in Honolulu, Hawaii. *Water Research* **114**, 122–134.

Habel, S., Fletcher, C. H., Rotzoll, K., El-Kadi, A. I. & Oki, D. S. 2019 Comparison of a simple hydrostatic and a data-intensive 3D numerical modeling method of simulating sea-level rise induced groundwater inundation for Honolulu, Hawai'i, USA. *Environmental Research Communications* **1** (4), 041005.

Hamlington, B. D., Strassburg, M. W., Leben, R. R., Han, W., Nerem, R. S. & Kim, K. Y. 2014 Uncovering an anthropogenic sea-level rise signal in the Pacific Ocean. *Nature Climate Change* **4** (9), 782–785.

Han, S. C., Sauber, J., Pollitz, F. & Ray, R. 2019 Sea level rise in the Samoan Islands escalated by viscoelastic relaxation after the 2009 Samoa-Tonga earthquake. *Journal of Geophysical Research: Solid Earth* **124** (4), 4142–4156.

Izuka, S. K., Engott, J. A., Rotzoll, K., Bassiouni, M., Johnson, A. G., Miller, L. D. & Mair, A. 2018 *Volcanic Aquifers of Hawai 'I – Hydrogeology, Water Budgets, and Conceptual Models (No. 2015-5164)*. US Geological Survey, Honolulu, HI, USA.

Kane, H. H., Fletcher, C. H., Frazer, L. N. & Barbee, M. M. 2015 Critical elevation levels for flooding due to sea-level rise in Hawai 'i. *Regional Environmental Change* **15** (8), 1679–1687.

Keener, V., Grecni, Z., Anderson Tagarino, K., Shuler, C. & Miles, W. 2021 *Climate Change in American Samoa: Indicators and Considerations for Key Sectors*. Report for the Pacific Islands Regional Climate Assessment. East-West Center, Honolulu, HI. Available from: https://eastwestcenter.org/PIRCA-AmericanSamoa.

Kluyver, T., Ragan-Kelley, B., Pérez, F., Granger, B. E., Bussonnier, M., Frederic, J., Kelley, K., Hamrick, J. B., Grout, J., Corlay, S., Ivanov, P. & Willing, C. 2016 Jupyter Notebooks-a publishing format for reproducible computational workflows. In *Positioning and Power in Academic Publishing: Players, Agents and Agendas* (Loizides, F. & Scmidt, B., eds.). IOS Press, Amsterdam, the Netherlands, pp. 87–90.

Knott, J. F., Elshaer, M., Daniel, J. S., Jacobs, J. M. & Kirshen, P. 2017 Assessing the effects of rising groundwater from sea level rise on the service life of pavements in coastal road infrastructure. *Transportation Research Record* **2639** (1), 1–10.

Ku, T. L., Kimmel, M. A., Easton, W. H. & O'Neil, T. J. 1974 Eustatic sea level 120,000 years ago on Oahu, Hawaii. *Science* **183** (4128), 959–962.

Kumar, L. & Taylor, S. 2015 Exposure of coastal built assets in the South Pacific to climate risks. *Nature Climate Change* **5** (11), 992–996.

Lu, X., Zhou, Y., Zhuang, Q., Prigent, C., Liu, Y. & Teuling, A. 2018 Increasing methane emissions from natural land ecosystems due to sea-level rise. *Journal of Geophysical Research: Biogeosciences* **123** (5), 1756–1768.

Maliva, R. 2021 *Climate Change and Groundwater: Planning and Adaptations for A Changing and Uncertain Future: WSP Methods in Water Resources Evaluation Series No. 6*. Springer Nature. https://doi.org/10.1007/978-3-030-66813-6.

Masterson, J. P., Fienen, M. N., Thieler, E. R., Gesch, D. B., Gutierrez, B. T. & Plant, N. G. 2014 Effects of sea-level rise on barrier island groundwater system dynamics–ecohydrological implications. *Ecohydrology* **7** (3), 1064–1071.

Muhs, D. R., Kennedy, G. L. & Rockwell, T. K. 1994 Uranium-series ages of marine terrace corals from the Pacific coast of North America and implications for last-interglacial sea level history. *Quaternary Research* **42** (1), 72–87.

Neumann, B., Vafeidis, A. T., Zimmermann, J. & Nicholls, R. J. 2015 Future coastal population growth and exposure to sea-level rise and coastal flooding-a global assessment. *PloS one* **10** (3), e0118571.

Nunn, P. D. & Mimura, N. 1997 Vulnerability of South Pacific island nations to sea-level rise. *Journal of Coastal Research* Special Issue no. **24**, 133–151.

Nunn, P. D., Klöck, C. & Duvat, V. 2021 Seawalls as maladaptations along island coasts. *Ocean & Coastal Management* **205**, 105554.

NWS – National Weather Service 2000 *Precipitation Records From 1971–2000*. Data Set. Available from: http://xmacis.rcc-acis.org (Accessed 20 July 2020).

OCM – Office for Coastal Management 2012 2012 NOAA American Samoa Lidar DEM: Islands of Tutuila, Aunu'u, Ofu, Olosega, Ta'u and Rose Atoll. Available from: https://www.fisheries.noaa.gov/inport/item/52876.

OCM – Office for Coastal Management 2016 NOAA Office for Coastal Management Sea Level Rise Data: 1-10ft Sea Level Rise Inundation Extent. Available from: https://www.fisheries.noaa.gov/inport/item/48106.

Plane, E., Hill, K. & May, C. 2019 A rapid assessment method to identify potential groundwater flooding hotspots as sea levels rise in coastal cities. *Water* **11** (11), 2228.

Rahimi, R., Tavakol-Davani, H., Graves, C., Gomez, A. & Fazel Valipour, M. 2020 Compound inundation impacts of coastal climate change: Sea-level rise, groundwater rise, and coastal precipitation. *Water* **12** (10), 2776.

Rotzoll, K. & Fletcher, C. H. 2013 Assessment of groundwater inundation as a consequence of sea-level rise. *Nature Climate Change* **3** (5), 477–481.

Shuler, C. K. 2019 *From Recharge to Reef: Assessing the Sources, Quantity, and Transport of Groundwater on Tutuila Island, American Samoa*. Doctoral dissertation, University of Hawai'i at Manoa.

Shuler, C. K. 2022 Data Repository: 2022 Hawai'i Cesspool Hazard Assessment & Prioritization Tool (Version v1) [Data set]. Zenodo. https://doi.org/10.5281/zenodo.7329880.

Shuler, C. K. & Mariner, K. E. 2020 Collaborative groundwater modeling: Open-source, cloud-based, applied science at a small-island water utility scale. *Environmental Modelling & Software* **127**, 104693.

Shuler, C., Brewington, L. & El-Kadi, A. I. 2021 A participatory approach to assessing groundwater recharge under future climate and land-cover scenarios, Tutuila, American Samoa. *Journal of Hydrology: Regional Studies* **34**, 100785.

Stearns, H. T. 1944 Geology of the Samoan islands. *Geological Society of America Bulletin* **55** (11), 1279–1332.

Suthersan, S. S. 2001 *Natural and Enhanced Remediation Systems*. CRC Press, Boca Raton, p. 440.

Szabo, B. J., Ludwig, K. R., Muhs, D. R. & Simmons, K. R. 1994 Thorium-230 ages of corals and duration of the last interglacial sea-level high stand on Oahu, Hawaii. *Science* **266** (5182), 93–96.

USGS – U.S. Geological Survey. 2018 *National Hydrography Dataset*. [Reston, Va.]. U.S. Dept. of the Interior, U.S. Geological Survey. Available from: https://www.usgs.gov/core-science-systems/ngp/national-hydrography.

Wang, Y. & Zhang, C. 2016 *Project Final Report - 21st Century High-Resolution Climate Projections for Guam and American Samoa*. Available from: https://www.sciencebase.gov/catalog/item/583331f6e4b046f05f211ae6 (Accessed 18 July 2020).

Werner, A. D. & Simmons, C. T. 2009 Impact of sea-level rise on sea water intrusion in coastal aquifers. *Ground Water* **47** (2), 197–204.

Whitall, D. R. & Holst, S. 2015 *Pollution in Surface Sediments in Faga'alu Bay, Tutuila, American Samoa*. NOAA Technical Memorandum NOS NCCOS 201, Silver Spring, MD, p. 54. doi:10.7289/V5/TM-NOS-NCCOS-201.

White, I., Falkland, T., Metutera, T., Metai, E., Overmars, M., Perez, P. & Dray, A. 2007 Climatic and human influences on groundwater in low atolls. *Vadose Zone J* **6** (3), 581–590.

First received 8 August 2023; accepted in revised form 9 November 2023. Available online 20 November 2023